

Results from the Hellenic Open University extensive air shower array

Stavros Nonis

School of Engineering, University of the Aegean, Chios, Greece

8th ICNFP 2019, 21-29 August 2019 Kolymbari, Crete, Greece

August 26, 2019



Results from the Hellenic Open University extensive air shower array

Stavros Nonis

School of Engineering, University of the Aegean, Chios, Greece

8th ICNFP 2019, 21-29 August 2019 Kolymbari, Crete, Greece

August 26, 2019



On behalf of the ASTRONEU group

- A. Leisos, A.G. Tsirigotis, G. Bourlis: Physics Laboratory, School of Science and Technology, Hellenic Open University.
- K. Papageorgiou, I. Gkialas : School of Engineering, University of the Aegean.
- S.E. Tzamarias, I. Manthos : Department of Physics, Aristotle University of Thessaloniki.

Outline

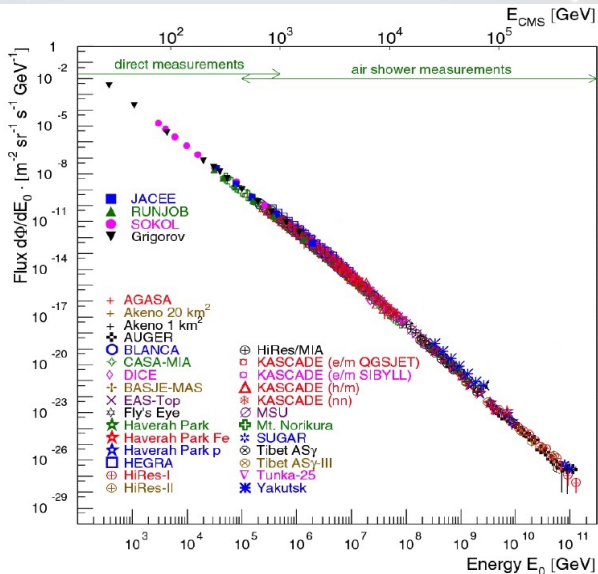
- 1 Cosmic Rays - Extensive air Showers (EAS)
- 2 Radio Emission
- 3 ASTRONUE Array
- 4 HDM's Performance
- 5 Event Selection-RF Analysis
- 6 Correlation Study and Combined Performance
- 7 Reconstructing EAS direction using RF signal from one antenna
- 8 Core-Energy- X_{max}
- 9 Conclusions and future work

Outline

- 1 Cosmic Rays - Extensive air Showers (EAS)
- 2 Radio Emission
- 3 ASTRONUE Array
- 4 HDM's Performance
- 5 Event Selection-RF Analysis
- 6 Correlation Study and Combined Performance
- 7 Reconstructing EAS direction using RF signal from one antenna
- 8 Core-Energy- X_{max}
- 9 Conclusions and future work

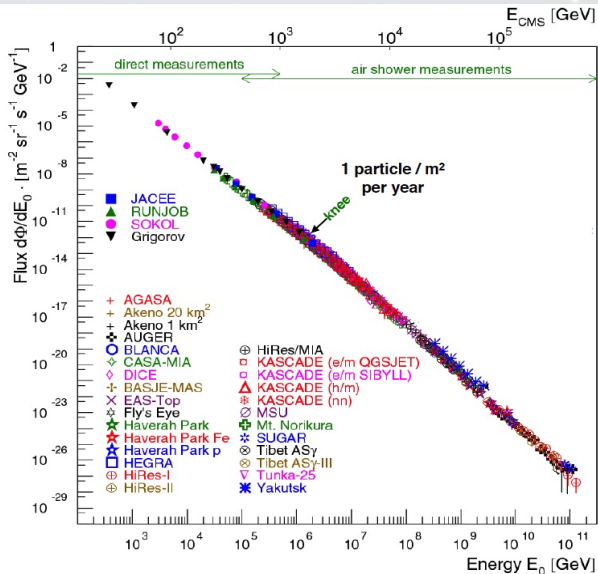
Cosmic Rays Spectrum

- Spectrum power law
 $dN/dE \sim E^{-3}$



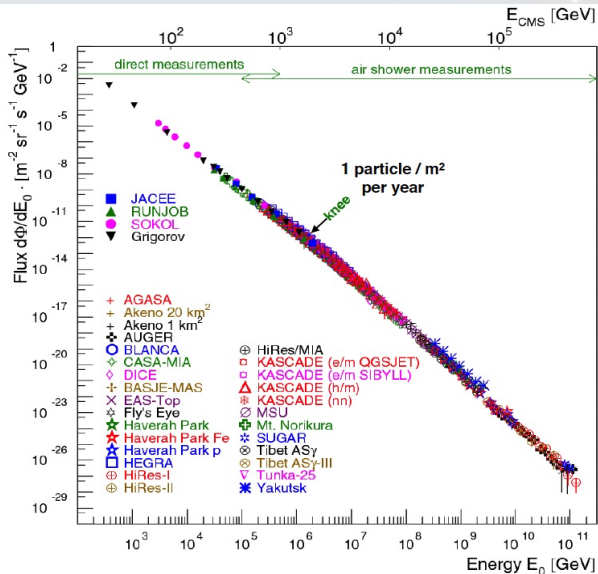
Cosmic Rays Spectrum

- Spectrum power law
 $dN/dE \sim E^{-3}$



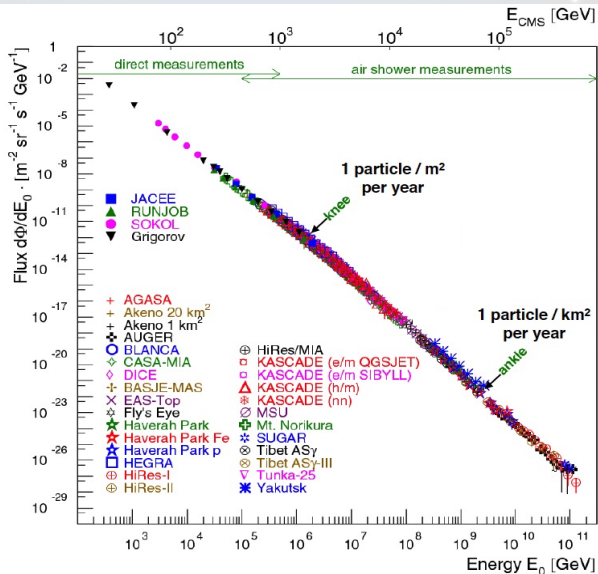
Cosmic Rays Spectrum

- Spectrum power law
 $dN/dE \sim E^{-3}$
- Up to the knee
galactic origin



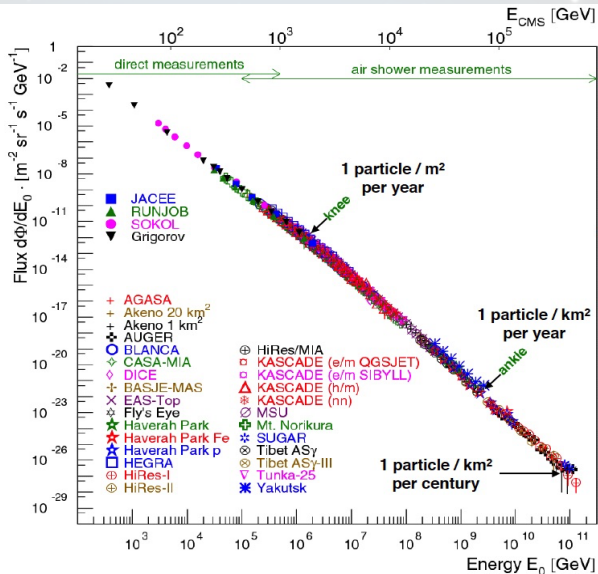
Cosmic Rays Spectrum

- Spectrum power law
 $dN/dE \sim E^{-3}$
- Up to the knee
galactic origin
- Beyond the ankle
extra galactic sources



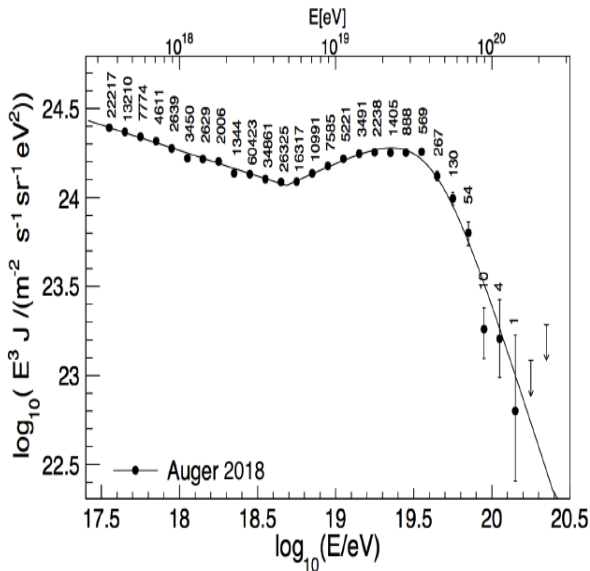
Cosmic Rays Spectrum

- Spectrum power law $dN/dE \sim E^{-3}$
- Up to the knee galactic origin
- Beyond the ankle extra galactic sources
- Clear cut off up to $6 \cdot 10^{19} \text{ eV}$



Cosmic Rays Spectrum

- Spectrum power law $dN/dE \sim E^{-3}$
- Up to the knee galactic origin
- Beyond the ankle extra galactic sources
- Clear cut off up to $6 \cdot 10^{19} eV$



Cosmic Rays - Open questions

- The nature of the Ultra High Energy Cosmic Rays p or Fe?

Cosmic Rays - Open questions

- The nature of the Ultra High Energy Cosmic Rays p or Fe?
- What are the sources?

Cosmic Rays - Open questions

- The nature of the Ultra High Energy Cosmic Rays p or Fe?
- What are the sources?
- Production mechanism?

Cosmic Rays - Open questions

- The nature of the Ultra High Energy Cosmic Rays p or Fe?
- What are the sources?
- Production mechanism?
- Galactic vs extra-galactic origin?

Cosmic Rays - Open questions

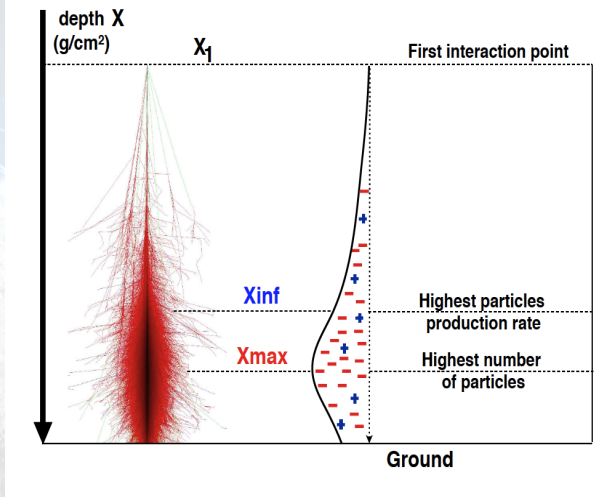
- The nature of the Ultra High Energy Cosmic Rays p or Fe?
- What are the sources?
- Production mechanism?
- Galactic vs extra-galactic origin?
- Why the spectrum at ultra-high energy fall out? GZK cutoff (only for p) or source limits?

Cosmic Rays - Open questions

- The nature of the Ultra High Energy Cosmic Rays p or Fe?
- What are the sources?
- Production mechanism?
- Galactic vs extra-galactic origin?
- Why the spectrum at ultra-high energy fall out? GZK cutoff (only for p) or source limits?
- Why the flux goes down dramatically? ($\text{Flux} / 10^3$ when energy $\cdot 10$).

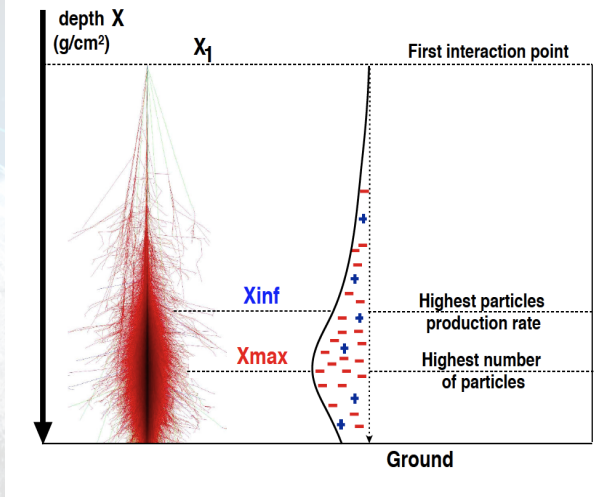
Extensive Air Showers (EAS)

- EAS: Cascade of particles.



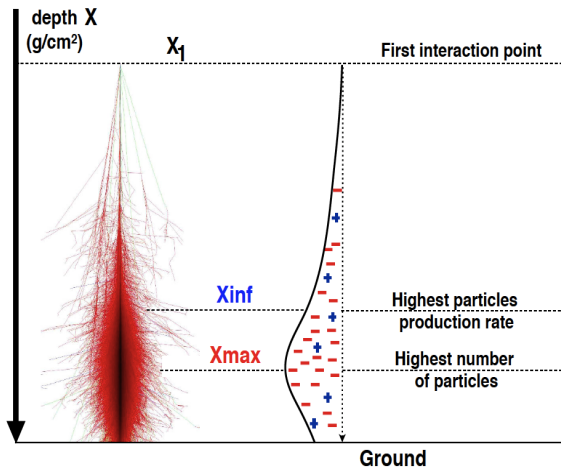
Extensive Air Showers (EAS)

- EAS: Cascade of particles.
- X_1 : particles creation is initiated.



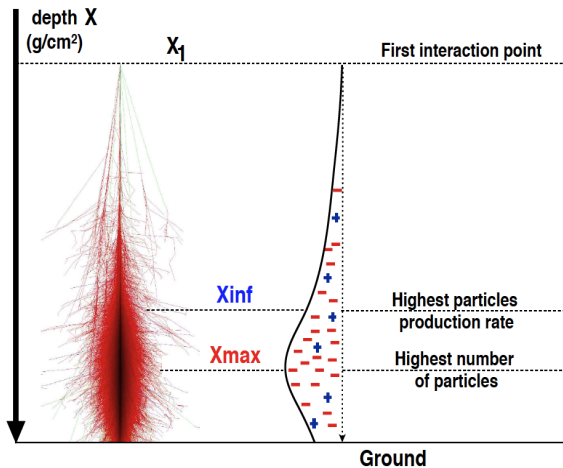
Extensive Air Showers (EAS)

- EAS: Cascade of particles.
- X_1 : particles creation is initiated.
- Longitudinal profile:
 $N_{particles}=f(X)$.



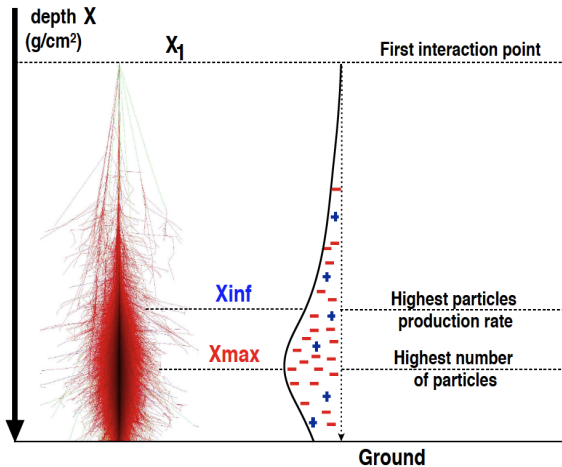
Extensive Air Showers (EAS)

- EAS: Cascade of particles.
- X_1 : particles creation is initiated.
- Longitudinal profile:
 $N_{particles}=f(X)$.
- X_{inf} : Inflection of the profile.



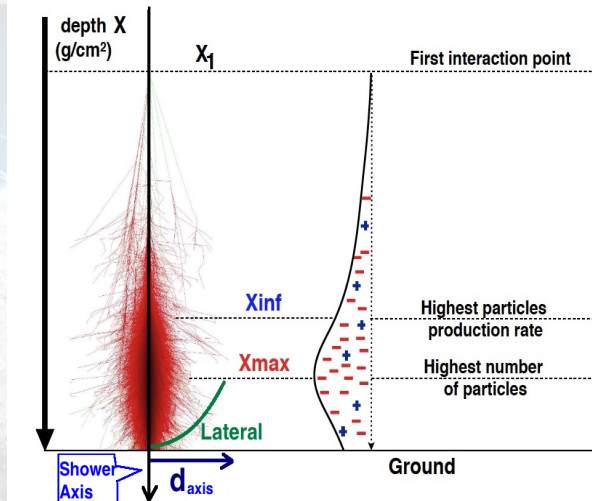
Extensive Air Showers (EAS)

- EAS: Cascade of particles.
- X_1 : particles creation is initiated.
- Longitudinal profile:
 $N_{particles}=f(X)$.
- X_{inf} : Inflection of the profile.
- X_{max} : Maximum number of particles.



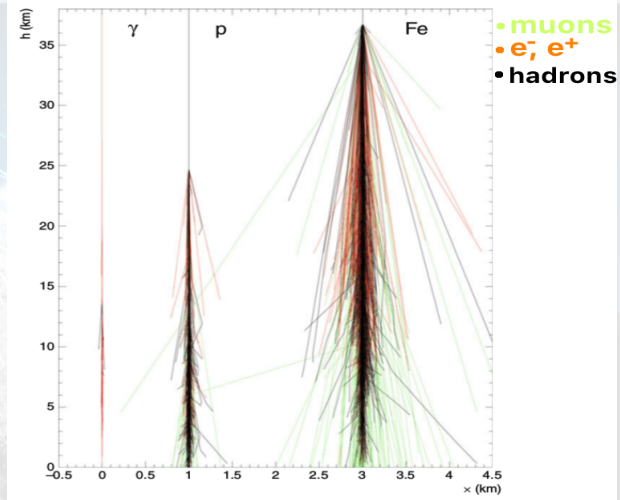
Extensive Air Showers (EAS)

- EAS: Cascade of particles.
- X_1 : particles creation is initiated.
- Longitudinal profile:
 $N_{particles} = f(X)$.
- X_{inf} : Inflection of the profile.
- X_{max} : Maximum number of particles.
- Lateral profile:
 $N = f(d_{axis})$.



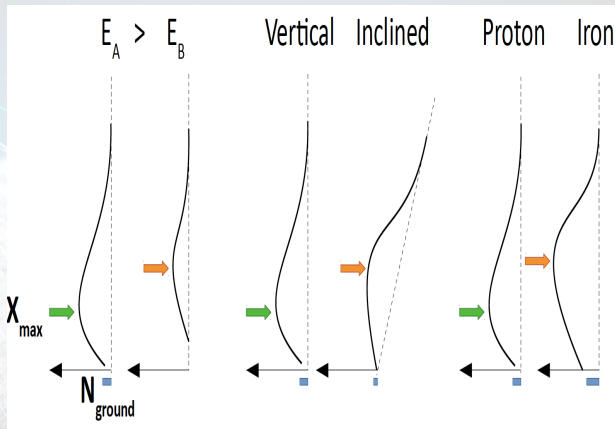
Extensive Air Showers (EAS)

- EAS: Cascade of particles.
- X_1 : particles creation is initiated.
- Longitudinal profile:
 $N_{particles}=f(X)$.
- X_{inf} : Inflection of the profile.
- X_{max} : Maximum number of particles.
- Lateral profile:
 $N = f(d_{axis})$.



Extensive Air Showers (EAS)

- EAS: Cascade of particles.
- X_1 : particles creation is initiated.
- Longitudinal profile:
 $N_{particles} = f(X)$.
- X_{inf} : Inflection of the profile.
- X_{max} : Maximum number of particles.
- Lateral profile:
 $N = f(d_{axis})$.
- Both profiles are correlated to **direction, energy, mass**



Outline

- 1 Cosmic Rays - Extensive air Showers (EAS)
- 2 Radio Emission**
- 3 ASTRONUE Array
- 4 HDM's Performance
- 5 Event Selection-RF Analysis
- 6 Correlation Study and Combined Performance
- 7 Reconstructing EAS direction using RF signal from one antenna
- 8 Core-Energy- X_{max}
- 9 Conclusions and future work

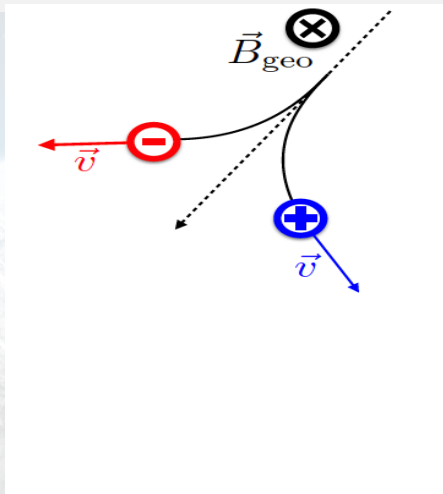
Geomagnetic effect

- Charges moving in the geomagnetic field.

¹ Kahn and Lerche 1966

Geomagnetic effect

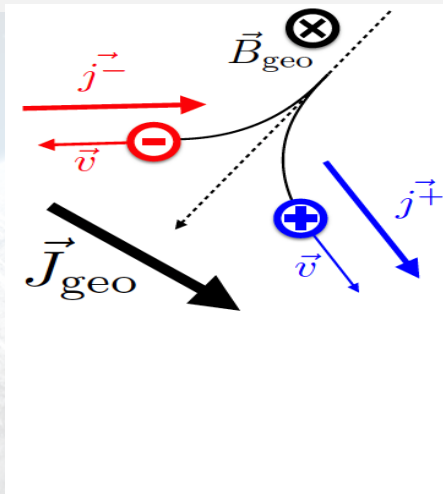
- Charges moving in the geomagnetic field.
- Lorentz force opposite deviation of e^- , e^+ .¹



¹ Kahn and Lerche 1966

Geomagnetic effect

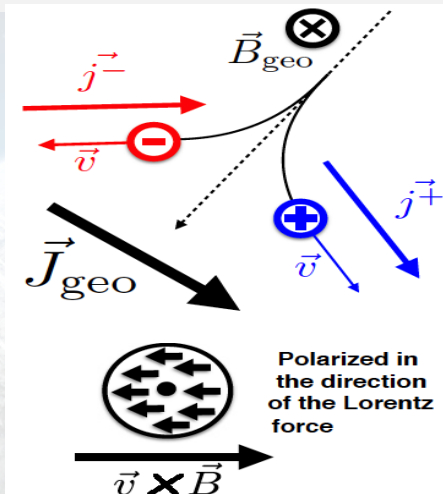
- Charges moving in the geomagnetic field.
- Lorenz force opposite deviation of e^- , e^+ .¹
- Transverse current (time variation).



¹ Kahn and Lerche 1966

Geomagnetic effect

- Charges moving in the geomagnetic field.
- Lorentz force opposite deviation of e^- , e^+ .¹
- Transverse current (time variation).
- Electric Field polarized in the direction $\vec{v} \times \vec{B}$.



¹ Kahn and Lerche 1966

Charge excess effect

- During shower development

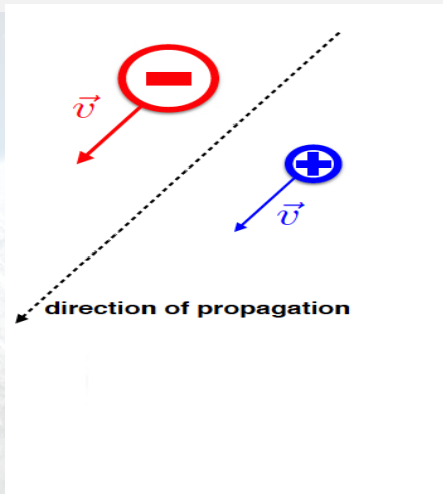
e^+ annihilate with e^- of the medium.



² Askaryan 1962

Charge excess effect

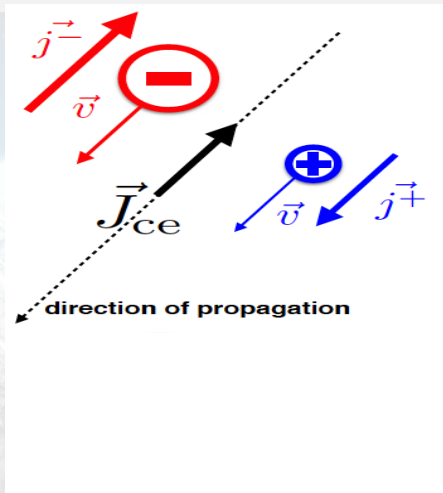
- During shower development e^+ annihilate with e^- of the medium.
- A negative charge excess.²



² Askaryan 1962

Charge excess effect

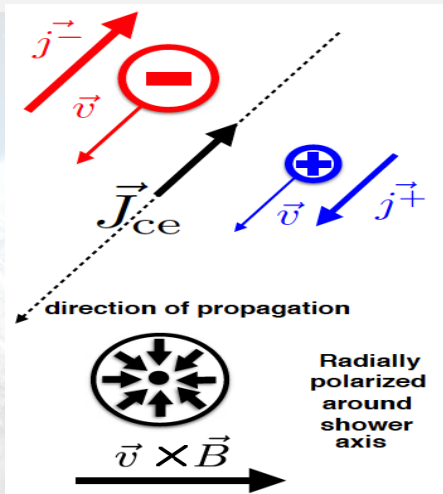
- During shower development e^+ annihilate with e^- of the medium.
- A negative charge excess.²
- Current // to shower axis.



² Askaryan 1962

Charge excess effect

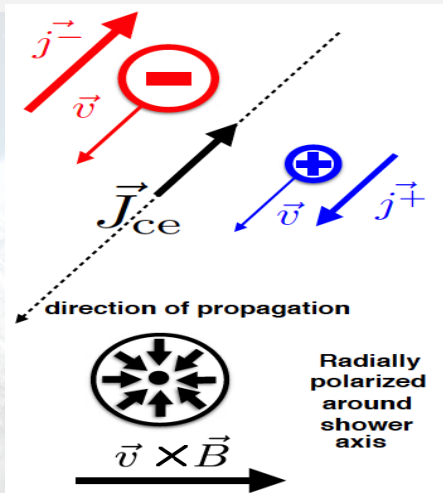
- During shower development e^+ annihilate with e^- of the medium.
- A negative charge excess.²
- Current // to shower axis.
- Electric Field radially polarized around the shower axis.



² Askaryan 1962

Charge excess effect

- During shower development e^+ annihilate with e^- of the medium.
- A negative charge excess.²
- Current // to shower axis.
- Electric Field radially polarized around the shower axis.
- The amplitude and the polarization pattern of the 2 contributions depends on the shower direction. The geomagnetic effect usually dominates.



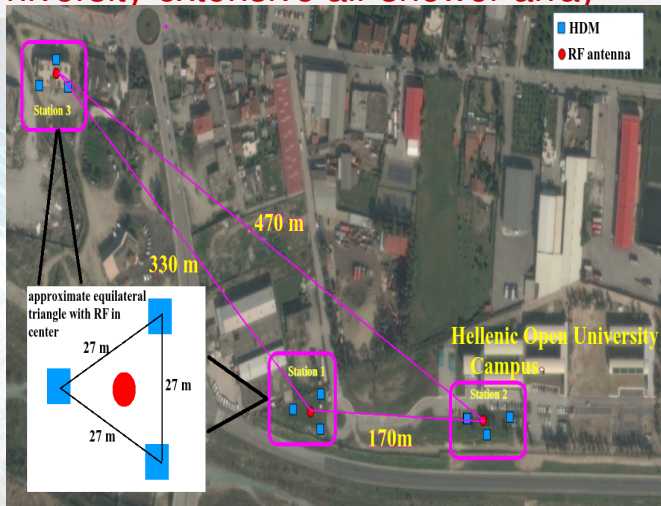
² Askaryan 1962

Outline

- 1 Cosmic Rays - Extensive air Showers (EAS)
- 2 Radio Emission
- 3 **ASTRONUE Array**
- 4 HDM's Performance
- 5 Event Selection-RF Analysis
- 6 Correlation Study and Combined Performance
- 7 Reconstructing EAS direction using RF signal from one antenna
- 8 Core-Energy- X_{max}
- 9 Conclusions and future work

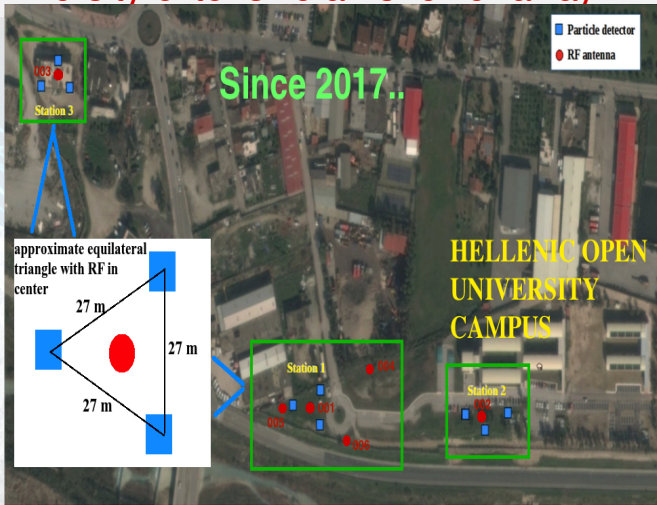
Hellenic Open University extensive air shower array

- **ASTRONEU: SD and RF array**
(3 stations) developed in the campus of the HOU.



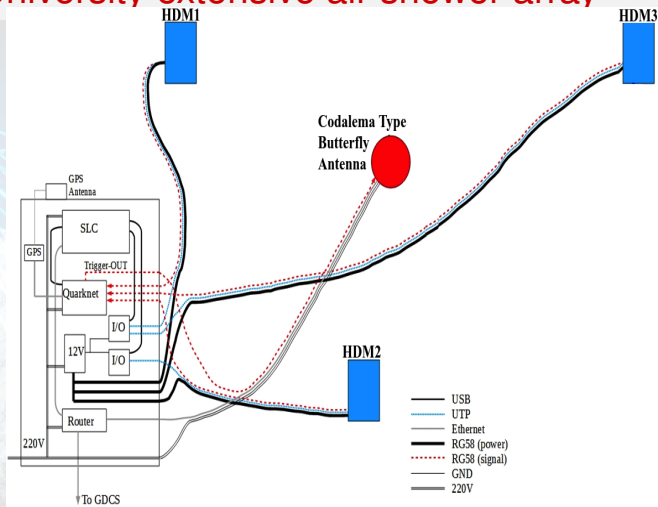
Hellenic Open University extensive air shower array

- **ASTRONUE: SD and RF array**
(3 stations) developed in the campus of the HOU.



Hellenic Open University extensive air shower array

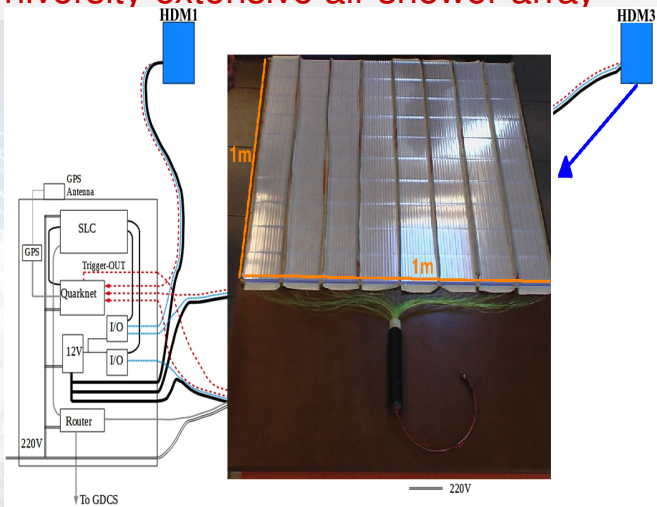
- **ASTRONEU: SD and RF array**
(3 stations) developed in the campus of the HOU.
- Each station includes 3 **HELICON Detector Modules (HDM) SD + 1 Codalema type 2 dipole Butterfly antenna (BF) + LNA.**³



³ arXiv:1702.04902 [physics.ins-det]

Hellenic Open University extensive air shower array

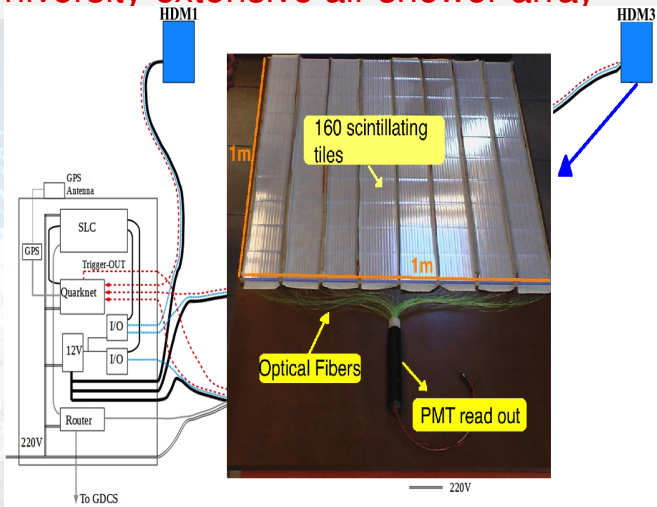
- **ASTRONEU: SD and RF array** (3 stations) developed in the campus of the HOU.
- Each station includes 3 **HELICON Detector Modules (HDM) SD + 1 Codalema type 2 dipole Butterfly antenna (BF) + LNA.**³



³ arXiv:1702.04902 [physics.ins-det]

Hellenic Open University extensive air shower array

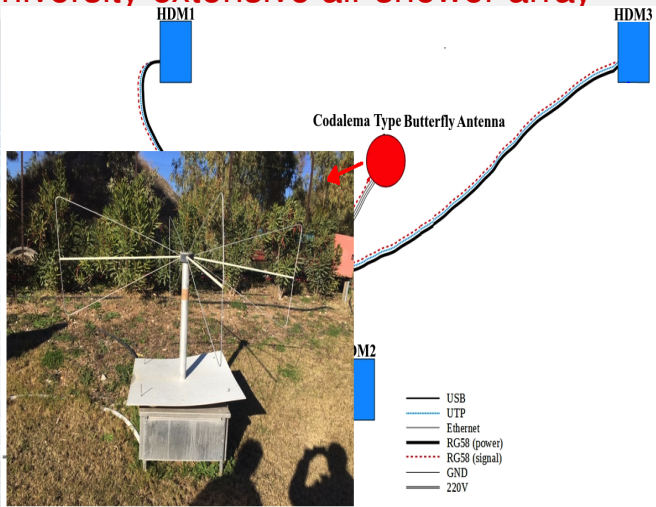
- **ASTRONEU: SD and RF array** (3 stations) developed in the campus of the HOU.
- Each station includes 3 **HELICON Detector Modules (HDM) SD + 1 Codalema type 2 dipole Butterfly antenna (BF) + LNA.**³



³ arXiv:1702.04902 [physics.ins-det]

Hellenic Open University extensive air shower array

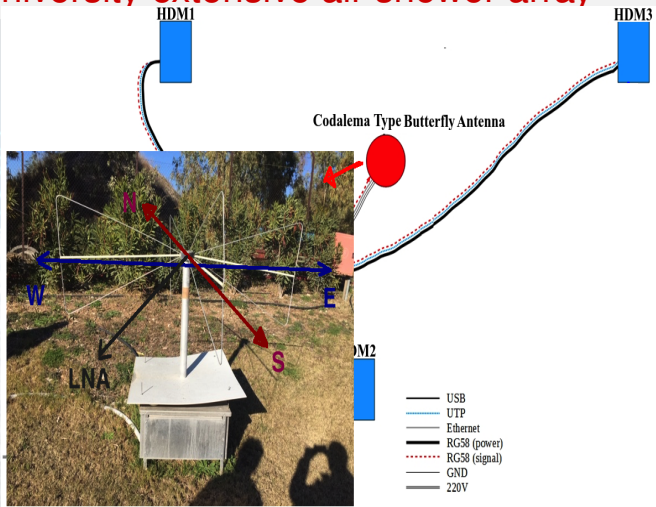
- **ASTRONEU: SD and RF array** (3 stations) developed in the campus of the HOU.
- Each station includes 3 **HELYCON Detector Modules (HDM) SD + 1 Codalema type 2 dipole Butterfly antenna (BF) + LNA.**³



³ arXiv:1702.04902 [physics.ins-det]

Hellenic Open University extensive air shower array

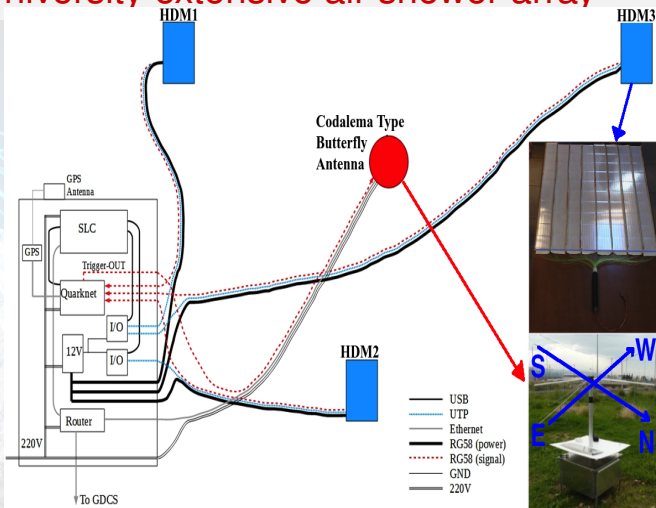
- **ASTRONEU: SD and RF array** (3 stations) developed in the campus of the HOU.
- Each station includes 3 **HELICON Detector Modules (HDM) SD + 1 Codalema type 2 dipole Butterfly antenna (BF) + LNA.**³



³ arXiv:1702.04902 [physics.ins-det]

Hellenic Open University extensive air shower array

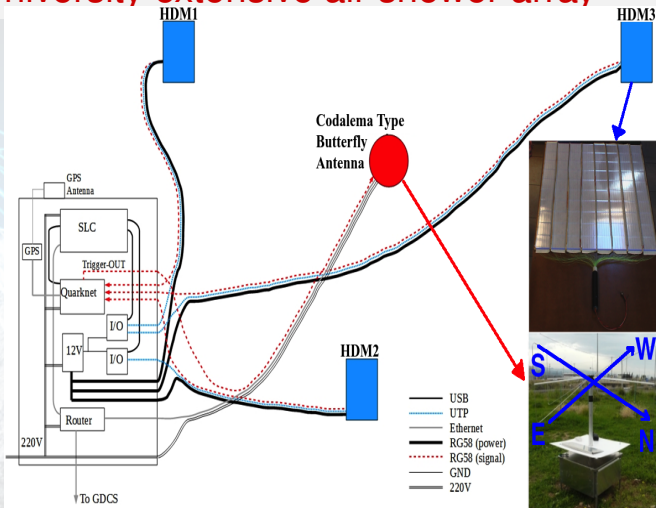
- **ASTRONEU: SD and RF array** (3 stations) developed in the campus of the HOU.
- Each station includes 3 **HELICON Detector Modules (HDM) SD + 1 Codalema type 2 dipole Butterfly antenna (BF) + LNA.**³
- Station triggers when all HDM acquire a threshold signal and activates the BFA recording.



³ arXiv:1702.04902 [physics.ins-det]

Hellenic Open University extensive air shower array

- **ASTRONEU: SD and RF array** (3 stations) developed in the campus of the HOU.
- Each station includes 3 **HELYCON Detector Modules (HDM) SD + 1 Codalema type 2 dipole Butterfly antenna (BF) + LNA.**³
- Station triggers when all HDM acquire a threshold signal and activates the BFA recording.
- **ASTRONEU CR telescope operates in an urban environment.**



³ arXiv:1702.04902 [physics.ins-det]

Outline

- 1 Cosmic Rays - Extensive air Showers (EAS)
- 2 Radio Emission
- 3 ASTRONUE Array
- 4 HDM's Performance**
- 5 Event Selection-RF Analysis
- 6 Correlation Study and Combined Performance
- 7 Reconstructing EAS direction using RF signal from one antenna
- 8 Core-Energy- X_{max}
- 9 Conclusions and future work

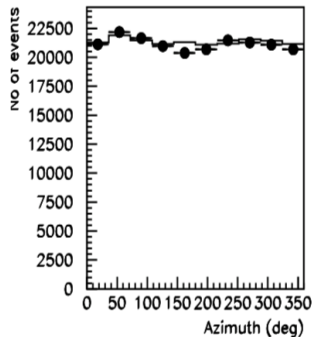
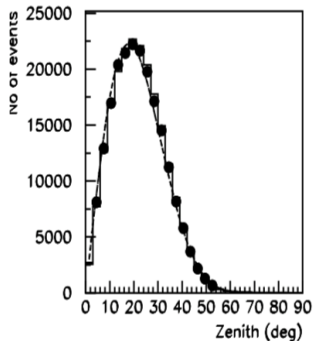
Performance of the stations

- Results for the evaluation of the HDM's performance of the 3 stations.⁴

⁴ arXiv:1801.04768 [physics.ins-det]

Performance of the stations

- Results for the evaluation of the HDM's performance of the 3 stations.⁴
- Event rates, Angular Resolution, Energy Threshold.



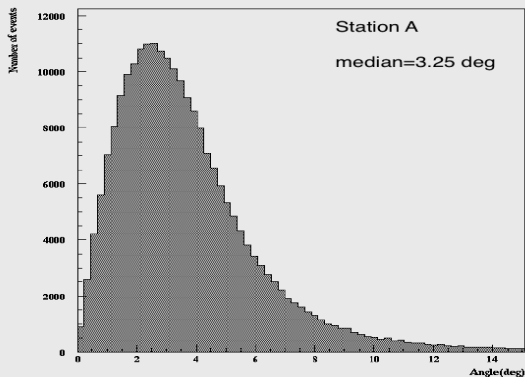
station	Event Rate (hr ⁻¹)	σ_{θ} (deg)	σ_{ϕ} (deg)	ω_{median} (deg)	E_{th} (TeV)
A	17.5	3.3	10.4	3.3	20
B	11.5	6.0	14.8	5.5	30
C	18.9	3.7	11.2	3.6	20

⁴ arXiv:1801.04768 [physics.ins-det]

Performance of the stations

- Results for the evaluation of the HDM's performance of the 3 stations.⁴

- Event rates, Angular Resolution, Energy Threshold.



station	Event Rate (hr ⁻¹)	σ_θ (deg)	σ_ϕ (deg)	ω_{median} (deg)	E_{th} (TeV)
A	17.5	3.3	10.4	3.3	20
B	11.5	6.0	14.8	5.5	30
C	18.9	3.7	11.2	3.6	20

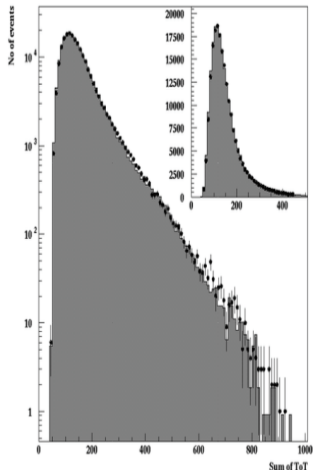
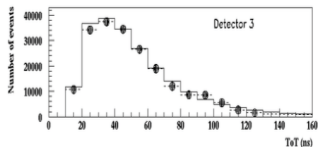
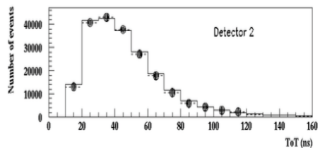
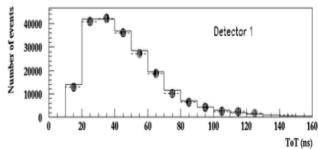
⁴ arXiv:1801.04768 [physics.ins-det]

Performance of the stations

- Results for the evaluation of the HDM's performance of the 3 stations. ⁴

- Event rates, Angular Resolution, Energy Threshold.

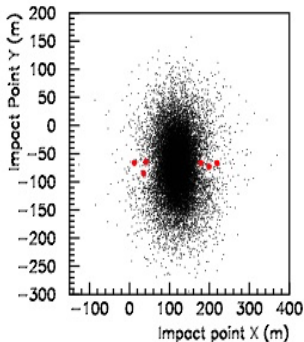
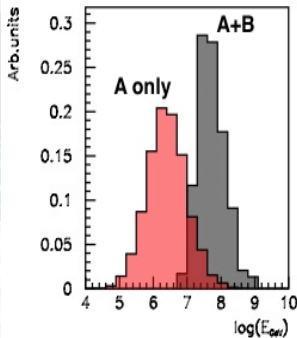
- ToT distribution for 3 HDM of station1.



⁴ arXiv:1801.04768 [physics.ins-det]

Performance of the stations

- Results for the evaluation of the HDM's performance of the 3 stations.⁴
- Event rates, Angular Resolution, Energy Threshold.
- ToT distribution for 3 HDM of station1.
- Energy and shower core distribution for MC events.



Station A+B: Energy Threshold $5 \cdot 10^3 \text{ TeV}$
 Angular resolution 2.9°
 Events rate 0.15 events/h

⁴ arXiv:1801.04768 [physics.ins-det]

Performance of the stations

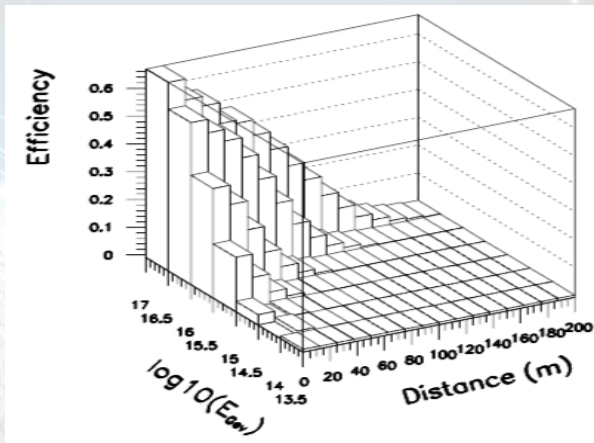
- Results for the evaluation of the HDM's performance of the 3 stations.⁴

- Event rates, Angular Resolution, Energy Threshold.

- ToT distribution for 3 HDM of station1.

- Energy and shower core distribution for MC events.

- Efficiency of HDM in detecting showers. Depends on shower core, energy. Max 60% for A.



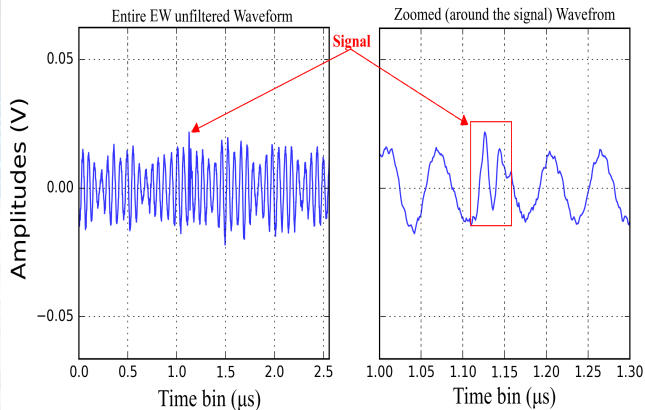
⁴ arXiv:1801.04768 [physics.ins-det]

Outline

- 1 Cosmic Rays - Extensive air Showers (EAS)
- 2 Radio Emission
- 3 ASTRONUE Array
- 4 HDM's Performance
- 5 Event Selection-RF Analysis**
- 6 Correlation Study and Combined Performance
- 7 Reconstructing EAS direction using RF signal from one antenna
- 8 Core-Energy- X_{max}
- 9 Conclusions and future work

RF signal characteristics⁵

- Intense peak localized in a time interval of 20-30ns

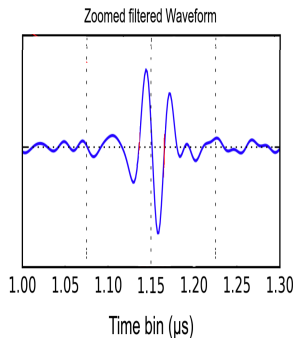
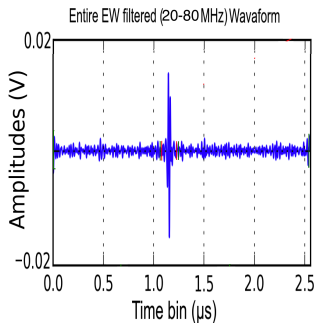


⁵ arXiv:1702.05794 [physics.ins-det]

⁶ Diego Torres Machado and the CODALEMA Collaboration 2013 J. Phys.: Conf. Ser. 409 012074

RF signal characteristics⁵

- Intense peak localized in a time interval of 20-30ns

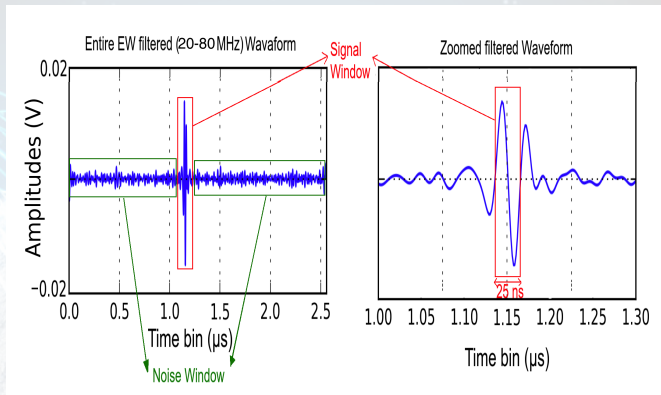


⁵ arXiv:1702.05794 [physics.ins-det]

⁶ Diego Torres Machado and the CODALEMA Collaboration 2013 J. Phys.: Conf. Ser. 409 012074

RF signal characteristics⁵

- Intense peak localized in a time interval of 20-30ns
- Signal to Noise Ratio (SNR) ≥ 8 .

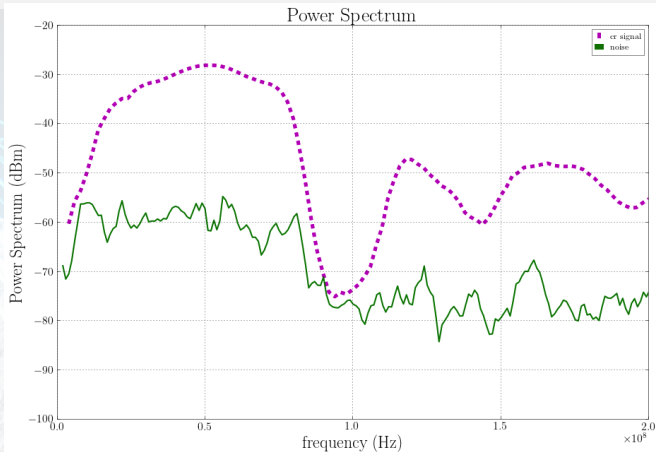


⁵ arXiv:1702.05794 [physics.ins-det]

⁶ Diego Torres Machado and the CODALEMA Collaboration 2013 J. Phys.: Conf. Ser. 409 012074

RF signal characteristics⁵

- Intense peak localized in a time interval of 20-30ns
- Signal to Noise Ratio (SNR) ≥ 8 .
- Power Spectrum smooth in 30-80MHz.

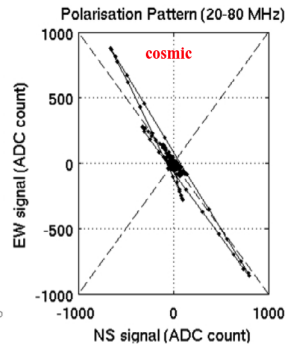
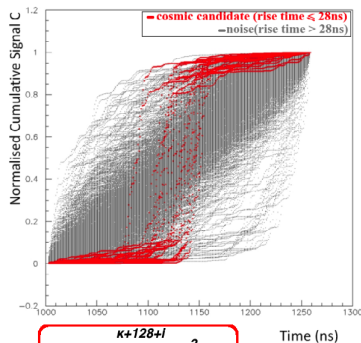


⁵ arXiv:1702.05794 [physics.ins-det]

⁶ Diego Torres Machado and the CODALEMA Collaboration 2013 J. Phys.: Conf. Ser. 409 012074

RF signal characteristics⁵

- Intense peak localized in a time interval of 20-30ns
- Signal to Noise Ratio (SNR) ≥ 8 .
- Power Spectrum smooth in 30-80MHz.
- Exhibits short signal rise time (≤ 28 ns)⁶.



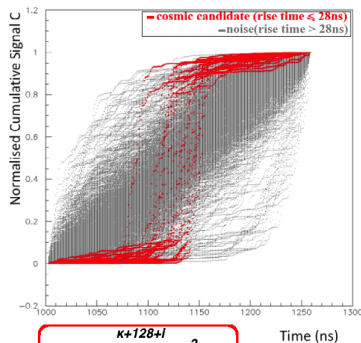
$$C(i) = \frac{\sum_{k=128}^{\kappa+128+i} E_{field}^2}{\sum_{k=128}^{\kappa+128} E_{field}^2} \quad k: \text{buffer bin signal max}$$

⁵ arXiv:1702.05794 [physics.ins-det]

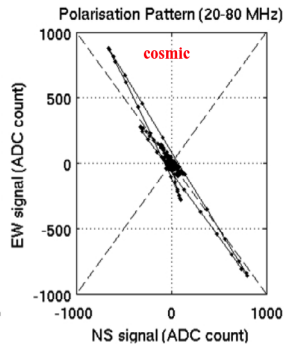
⁶ Diego Torres Machado and the CODALEMA Collaboration 2013 J. Phys.: Conf. Ser. 409 012074

RF signal characteristics⁵

- Intense peak localized in a time interval of 20-30ns
- Signal to Noise Ratio (SNR) ≥ 8 .
- Power Spectrum smooth in 30-80MHz.
- Exhibits short signal rise time (≤ 28 ns)⁶.
- Polarization approximately linear.



$$C(i) = \frac{\sum_{k=128}^{\kappa+128+i} E_{field}^2}{\sum_{k=128}^{\kappa+128} E_{field}^2} \quad k: \text{buffer bin signal max}$$

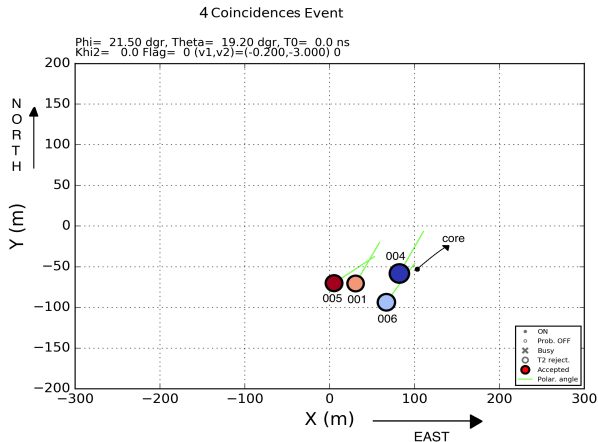


⁵ arXiv:1702.05794 [physics.ins-det]

⁶ Diego Torres Machado and the CODALEMA Collaboration 2013 J. Phys.: Conf. Ser. 409 012074

RF signal characteristics⁵

- Intense peak localized in a time interval of 20-30ns
- Signal to Noise Ratio (SNR) ≥ 8 .
- Power Spectrum smooth in 30-80MHz.
- Exhibits short signal rise time (≤ 28 ns)⁶.
- Polarization approximately linear.
- 4 Coincidences event Station A.

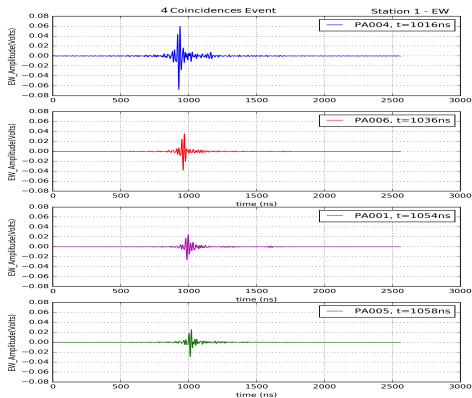


⁵ arXiv:1702.05794 [physics.ins-det]

⁶ Diego Torres Machado and the CODALEMA Collaboration 2013 J. Phys.: Conf. Ser. 409 012074

RF signal characteristics⁵

- Intense peak localized in a time interval of 20-30ns
- Signal to Noise Ratio (SNR) ≥ 8 .
- Power Spectrum smooth in 30-80MHz.
- Exhibits short signal rise time (≤ 28 ns)⁶.
- Polarization approximately linear.
- 4 Coincidences event Station A.

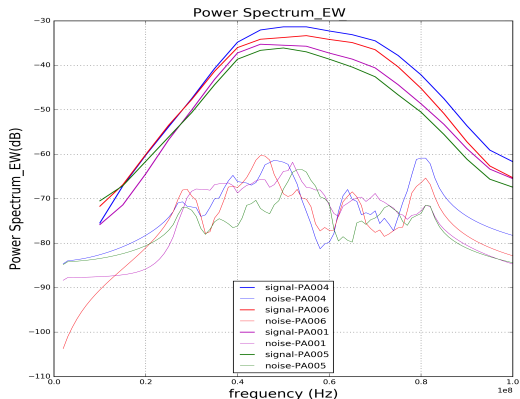


⁵ arXiv:1702.05794 [physics.ins-det]

⁶ Diego Torres Machado and the CODALEMA Collaboration 2013 J. Phys.: Conf. Ser. 409 012074

RF signal characteristics⁵

- Intense peak localized in a time interval of 20-30ns
- Signal to Noise Ratio (SNR) ≥ 8 .
- Power Spectrum smooth in 30-80MHz.
- Exhibits short signal rise time (≤ 28 ns)⁶.
- Polarization approximately linear.
- 4 Coincidences event Station A.

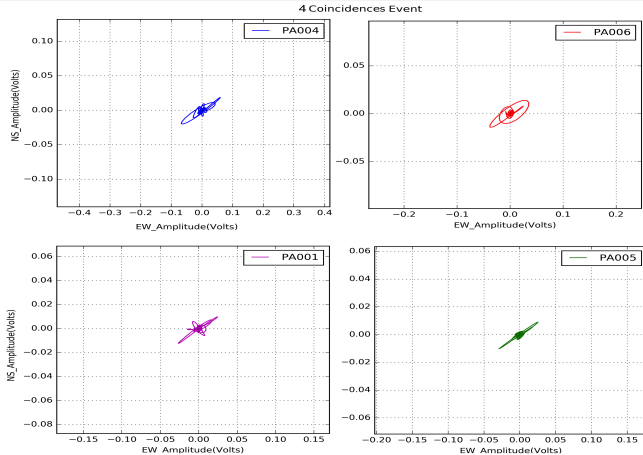


⁵ arXiv:1702.05794 [physics.ins-det]

⁶ Diego Torres Machado and the CODALEMA Collaboration 2013 J. Phys.: Conf. Ser. 409 012074

RF signal characteristics⁵

- Intense peak localized in a time interval of 20-30ns
- Signal to Noise Ratio (SNR) ≥ 8 .
- Power Spectrum smooth in 30-80MHz.
- Exhibits short signal rise time (≤ 28 ns)⁶.
- Polarization approximately linear.
- 4 Coincidences event Station A.



⁵ arXiv:1702.05794 [physics.ins-det]

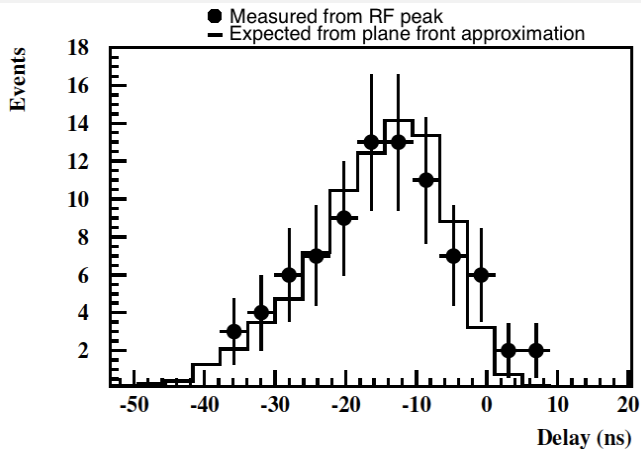
⁶ Diego Torres Machado and the CODALEMA Collaboration 2013 J. Phys.: Conf. Ser. 409 012074

Outline

- 1 Cosmic Rays - Extensive air Showers (EAS)
- 2 Radio Emission
- 3 ASTRONUE Array
- 4 HDM's Performance
- 5 Event Selection-RF Analysis
- 6 Correlation Study and Combined Performance**
- 7 Reconstructing EAS direction using RF signal from one antenna
- 8 Core-Energy- X_{max}
- 9 Conclusions and future work

RF signal timing - Electric Field vs Energy distribution

- RF signal timing using direction from HDMs vs using the peak of the EW RF pulse.⁵

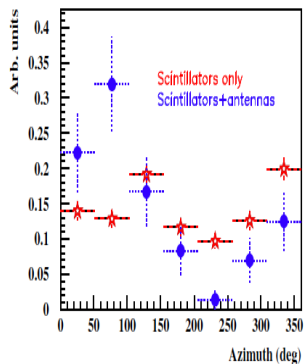
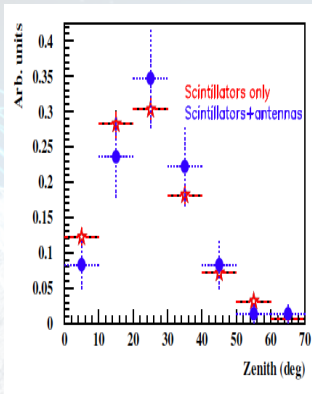


⁷ Leisos, A et al., Hybrid Detection of High Energy Showers in Urban Environments, Universe 2019 5(1) 3.

⁸ Vincent Marin and Benoît Revenu. Astropart. Phys., 35 (2012) 733.

RF signal timing - Electric Field vs Energy distribution

- RF signal timing using direction from HDMs vs using the peak of the EW RF pulse.⁵
- Showers axis direction using only HDM and both HDM & BFA

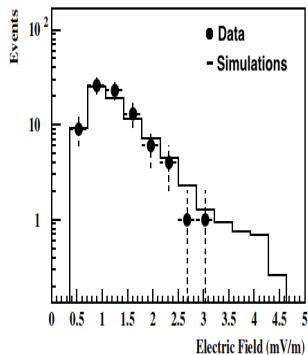
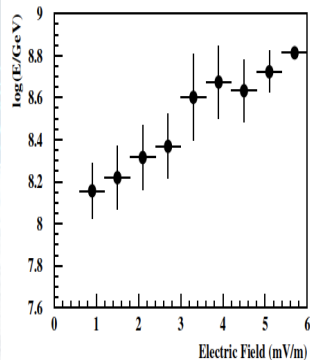


⁷ Leisos, A et al., Hybrid Detection of High Energy Showers in Urban Environments, Universe 2019 5(1) 3.

⁸ Vincent Marin and Benoît Revenu. Astropart. Phys., 35 (2012) 733.

RF signal timing - Electric Field vs Energy distribution

- RF signal timing using direction from HDMs vs using the peak of the EW RF pulse.⁵
- Showers axis direction using only HDM and both HDM & BFA
- SELFAS⁶ package predict the electric field for MC events. Electric field as a function of the energy.

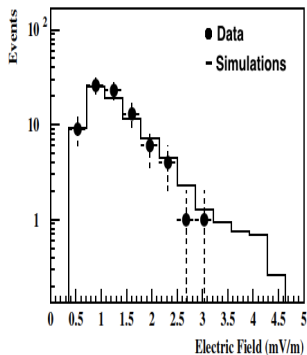
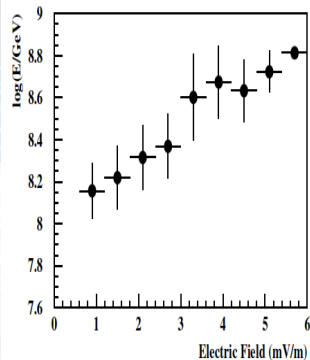


⁷ Leisos, A et al., Hybrid Detection of High Energy Showers in Urban Environments, Universe 2019 5(1) 3.

⁸ Vincent Marin and Benoît Revenu. Astropart. Phys., 35 (2012) 733.

RF signal timing - Electric Field vs Energy distribution

- RF signal timing using direction from HDMs vs using the peak of the EW RF pulse.⁵
- Showers axis direction using only HDM and both HDM & BFA
- SELFAS⁶ package predict the electric field for MC events. Electric field as a function of the energy.
- Electric field intensity from RF data in good agreement with the simulations.



⁷ Leisos, A et al., Hybrid Detection of High Energy Showers in Urban Environments, Universe 2019 5(1) 3.

⁸ Vincent Marin and Benoît Revenu. Astropart. Phys., 35 (2012) 733.

Outline

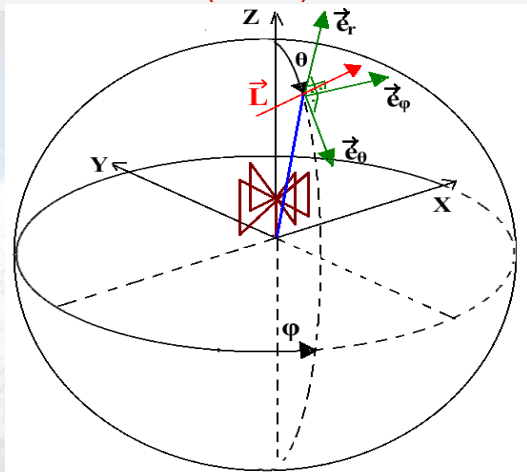
- 1 Cosmic Rays - Extensive air Showers (EAS)
- 2 Radio Emission
- 3 ASTRONUE Array
- 4 HDM's Performance
- 5 Event Selection-RF Analysis
- 6 Correlation Study and Combined Performance
- 7 Reconstructing EAS direction using RF signal from one antenna**
- 8 Core-Energy- X_{max}
- 9 Conclusions and future work

VEL - Voltage Response Model (VRM)

- Antenna+LNA Vector

Effective Length (L):

$$L = \frac{V_{LNA}}{E_{field}}$$



9

G. Burke and A. Poggio, NEC method of moments, parts I, II, III, tech. rep., (Lawrence Livermore National Laboratory, NEC-3, 1983).

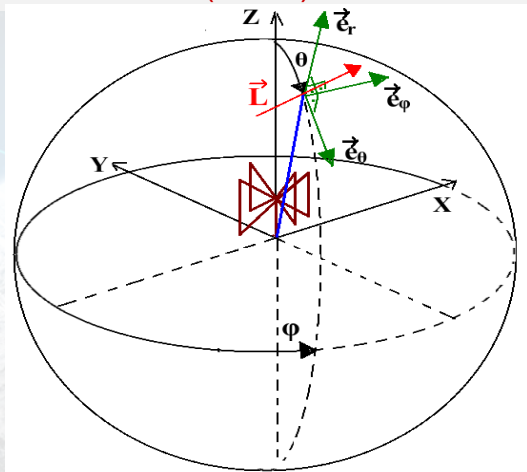
VEL - Voltage Response Model (VRM)

- Antenna+LNA Vector

Effective Length (L):

$$L = \frac{V_{LNA}}{E_{field}}$$

- VEL depends from the gain (frequency, zenith, azimuth)+structural features.



VEL - Voltage Response Model (VRM)

- Antenna+LNA Vector

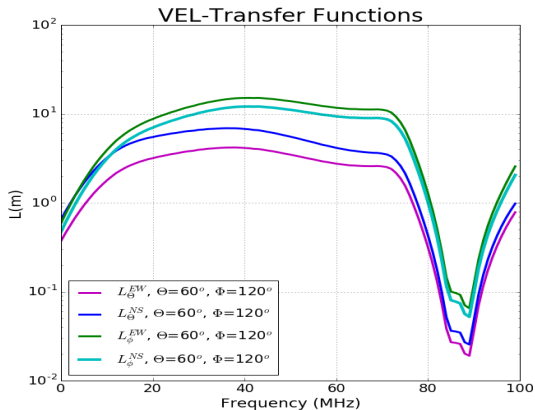
Effective Length (L):

$$L = \frac{V_{LNA}}{E_{field}}$$

- VEL depends from the gain

(frequency, zenith, azimuth)+structural features.

- NEC⁷ simulations for VEL.



VEL - Voltage Response Model (VRM)

Antenna+LNA Vector

Effective Length (L):

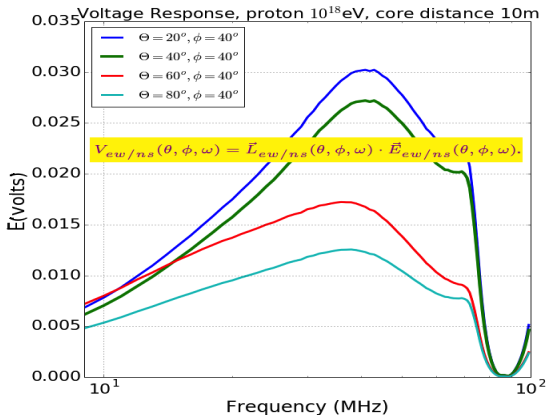
$$L = \frac{V_{LNA}}{E_{field}}$$

VEL depends from the gain

(frequency, zenith, azimuth)+structural features.

NEC⁷ simulations for VEL.

VRM of the RF to an incident electric field from direction (θ, ϕ) .



VEL - Voltage Response Model (VRM)

Antenna+LNA Vector

Effective Length (L):

$$L = \frac{V_{LNA}}{E_{field}}$$

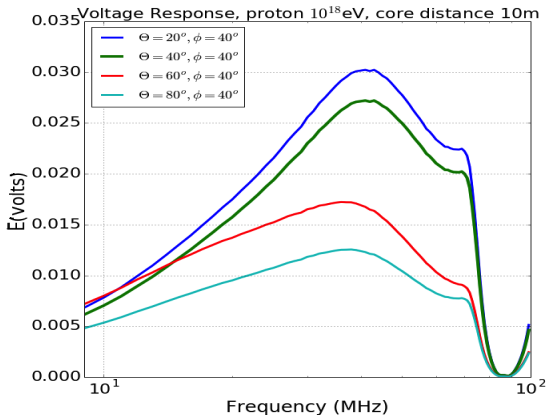
VEL depends from the gain

(frequency, zenith, azimuth)+structural features.

NEC⁷ simulations for VEL.

VRM of the RF to an incident electric field from direction (θ, ϕ) .

VRM for the RF system combining NEC+SELFAS.



⁹

G. Burke and A. Poggio, NEC method of moments, parts I, II, III, tech. rep., (Lawrence Livermore National Laboratory, NEC-3, 1983).

Estimation of the CR arrival direction

- Fitting the spectrum of a real cosmic event and the VRM which is calculated for different (θ, ϕ) .

$$\chi^2 = \sum_{30-80 \text{ MHz}} (a \cdot V_{\text{response}}(\theta, \phi, \omega) - V_{\text{real}}(\theta, \phi, \omega))^2$$

¹⁰ Nonis, S et al., EPJ Web Conf., 210, 05010 (2019).

Estimation of the CR arrival direction

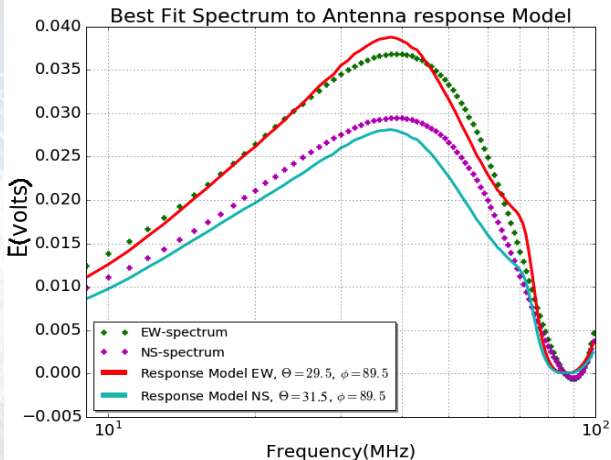
- Fitting the spectrum of a real cosmic event and the VRM which is calculated for different (θ, ϕ) .
- Minimizing the χ^2 .

$$\chi^2 = \sum_{30-80 \text{ MHz}} (a \cdot V_{\text{response}}(\theta, \phi, \omega) - V_{\text{real}}(\theta, \phi, \omega))^2$$

¹⁰ Nonis, S et al., EPJ Web Conf., 210, 05010 (2019).

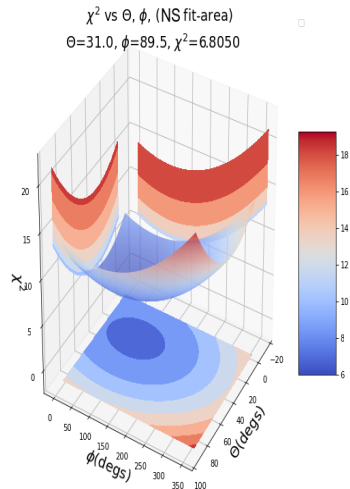
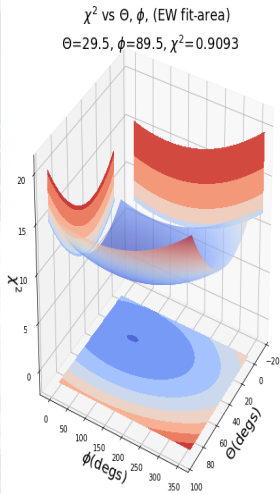
Estimation of the CR arrival direction

- Fitting the spectrum of a real cosmic event and the VRM which is calculated for different (θ, ϕ) .
- Minimizing the χ^2 .



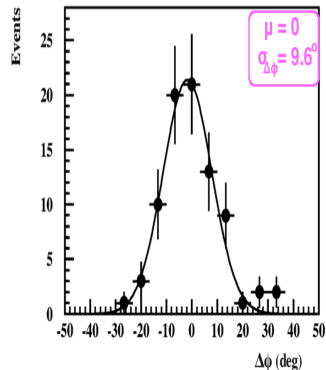
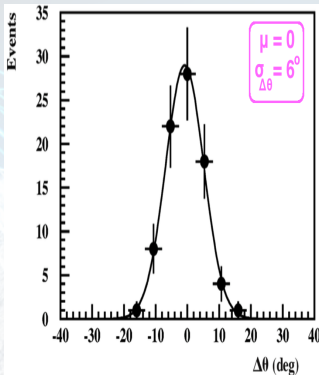
Estimation of the CR arrival direction

- Fitting the spectrum of a real cosmic event and the VRM which is calculated for different (θ, ϕ) .
- Minimizing the χ^2 .
- Fit the calculated $\chi^2 = f(\theta, \phi)$ with a surface. In the total minimum we have θ_{arr}, ϕ_{arr} .



Estimation of the CR arrival direction

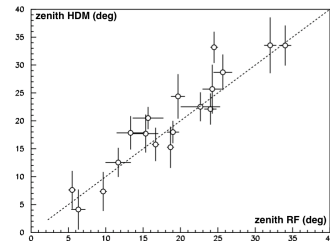
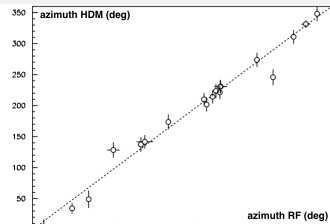
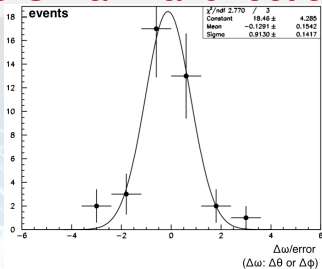
- Fitting the spectrum of a real cosmic event and the VRM which is calculated for different (θ, ϕ) .
- Minimizing the χ^2 .
- Fit the calculated $\chi^2 = f(\theta, \phi)$ with a surface. In the total minimum we have θ_{arr}, ϕ_{arr} .
- In previous work analyzed 92 events.⁸



¹⁰Nonis, S et al., EPJ Web Conf., 210, 05010 (2019).

Estimation of the CR arrival direction

- Fitting the spectrum of a real cosmic event and the VRM which is calculated for different (θ, ϕ) .
- Minimizing the χ^2 .
- Fit the calculated $\chi^2 = f(\theta, \phi)$ with a surface. In the total minimum we have θ_{arr}, ϕ_{arr} .
- In previous work analyzed 92 events.⁸
- Recently 19 events from 2,3 or 4 coincidences of the antennas in station A.

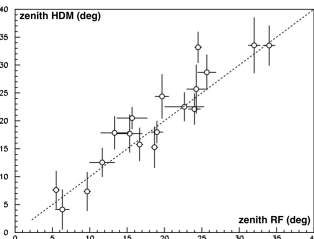
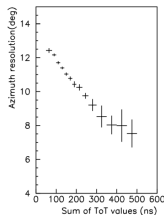
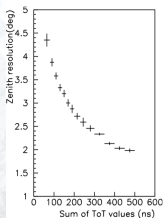
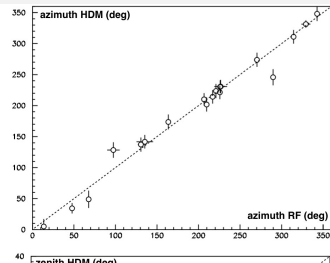
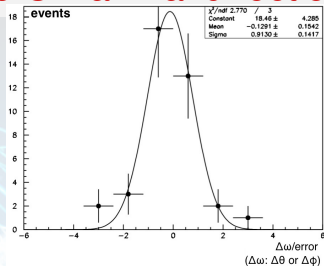


19 events with
2,3 or 4 antenna
coincidences compared
with HDM's arrival
reconstruction

¹⁰Nonis,S et al., EPJ Web Conf., 210, 05010 (2019).

Estimation of the CR arrival direction

- Fitting the spectrum of a real cosmic event and the VRM which is calculated for different (θ, ϕ) .
- Minimizing the χ^2 .
- Fit the calculated $\chi^2 = f(\theta, \phi)$ with a surface. In the total minimum we have θ_{arr}, ϕ_{arr} .
- In previous work analyzed 92 events.⁸
- Recently 19 events from 2,3 or 4 coincidences of the antennas in station A.



¹⁰Nonis,S et al., EPJ Web Conf., 210, 05010 (2019).

Outline

- 1 Cosmic Rays - Extensive air Showers (EAS)
- 2 Radio Emission
- 3 ASTRONUE Array
- 4 HDM's Performance
- 5 Event Selection-RF Analysis
- 6 Correlation Study and Combined Performance
- 7 Reconstructing EAS direction using RF signal from one antenna
- 8 Core-Energy- X_{max}**
- 9 Conclusions and future work

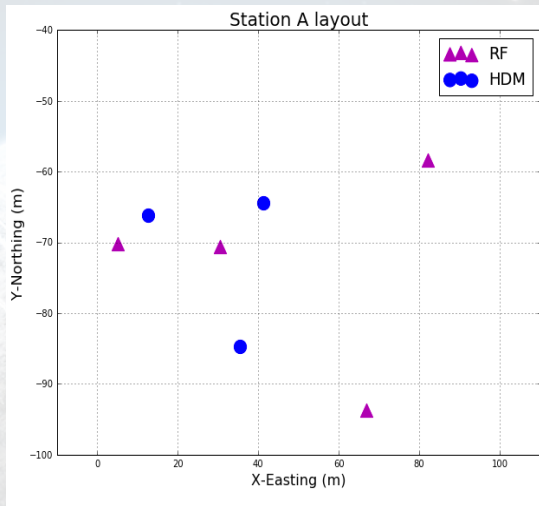
Reconstruction of main shower parameters - Tools

- Positions of counters and antennas of station-A.

Station	HDM position (x,y,z) (m)	RF position (x,y,z) (m)
A	(41.2, -64.4, 0.5)	(30.5, -70.6, 0.4)
	(35.4, -84.7, 0.3)	(82.1, -58.3, 1.1)
	(12.6, -66.2, 0.0)	(5.1, -70.2, 0.5)
		(66.8, -93.7, 1.0)

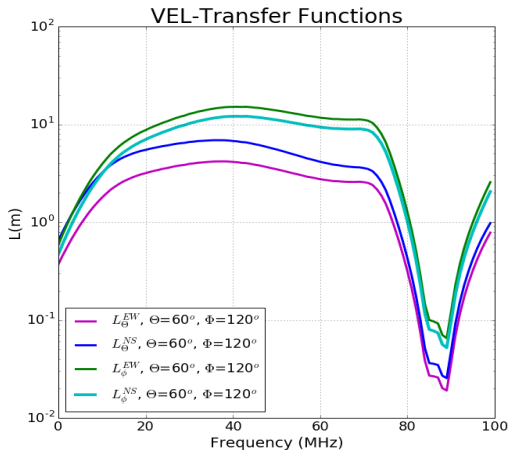
Reconstruction of main shower parameters - Tools

- Positions of counters and antennas of station-A.



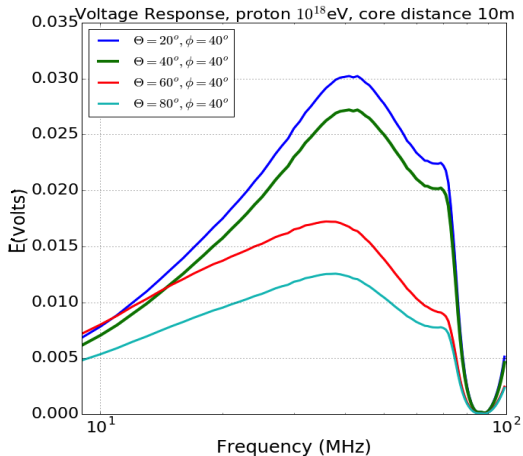
Reconstruction of main shower parameters - Tools

- Positions of counters and antennas of station-A.
- Voltage response V_{exp} , estimated from MC simulations (SELFAS+4nec2).



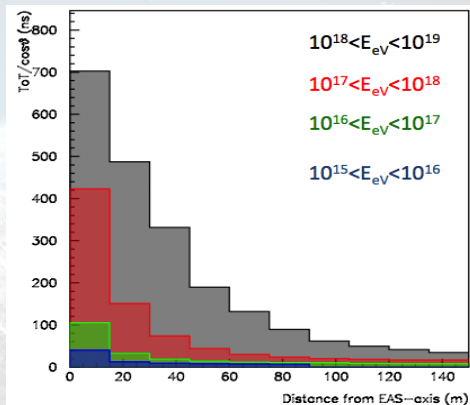
Reconstruction of main shower parameters - Tools

- Positions of counters and antennas of station-A.
- Voltage response V_{exp} , estimated from MC simulations (SELFAS+4nec2).



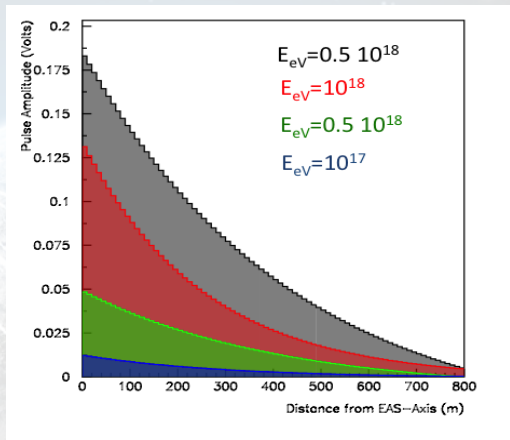
Reconstruction of main shower parameters - Tools

- Positions of counters and antennas of station-A.
- Voltage response V_{exp} , estimated from MC simulations (SELFAS+4nec2).
- Dependence of the ToT on the energy and distance from the EAS-axis.



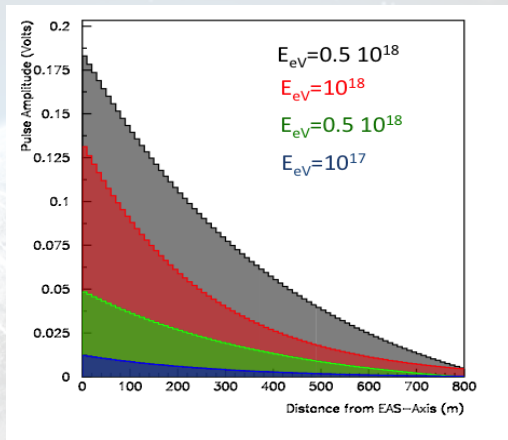
Reconstruction of main shower parameters - Tools

- Positions of counters and antennas of station-A.
- Voltage response V_{exp} , estimated from MC simulations (SELFAS+4nec2).
- Dependence of the ToT on the energy and distance from the EAS-axis.
- Dependence of the RF pulse amplitude on the energy and distance from the EAS-axis.



Reconstruction of main shower parameters - Tools

- Positions of counters and antennas of station-A.
- Voltage response V_{exp} , estimated from MC simulations (SELFAS+4nec2).
- Dependence of the ToT on the energy and distance from the EAS-axis.
- Dependence of the RF pulse amplitude on the energy and distance from the EAS-axis.
- This dependence can be used to estimate the EAS energy and the shower core position.



Reconstruction of main shower parameters - Method

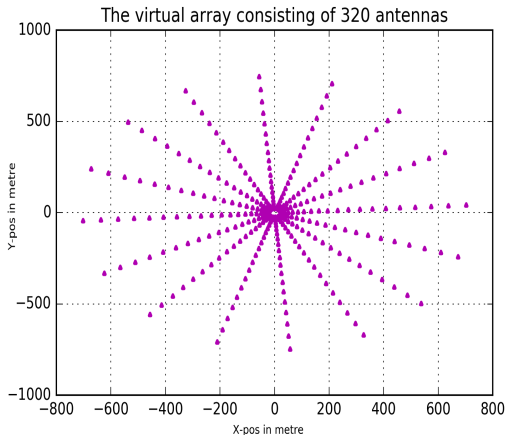
● RF data + simulations \rightarrow core, energy,

X_{max} with 4 antennas.



Reconstruction of main shower parameters - Method

- RF data + simulations \rightarrow core, energy, X_{max} with 4 antennas.
- Simulation of 60 showers for the virtual array for realistic X_1, X_{max}
 - 40 protons + 20 iron nuclei.
 - known arrival direction from measurement (timing and spectrum).
 - primary energy: 1EeV, fix core (0,0).



Reconstruction of main shower parameters - Method

- RF data + simulations \rightarrow core, energy, X_{max} with 4 antennas.
- Simulation of 60 showers for the virtual array for realistic X_1, X_{max}
 - 40 protons + 20 iron nuclei.
 - known arrival direction from measurement (timing and spectrum).
 - primary energy: 1EeV, fix core (0,0).
- For each core calculate χ^2 .

$$\chi^2(x_c, y_c, E, X_{max}) = \sum_{k=1}^4 \left(\frac{V_{\text{exp}}(x_c, y_c, E, X_{max}) - V_{\text{meas}}}{\sigma} \right)^2$$

Reconstruction of main shower parameters - Method

- RF data + simulations \rightarrow core, energy, X_{max} with 4 antennas.
- Simulation of 60 showers for the virtual array for realistic X_1, X_{max}
 - 40 protons + 20 iron nuclei.
 - known arrival direction from measurement (timing and spectrum).
 - primary energy: 1EeV, fix core (0,0).
- For each core calculate χ^2 .
- Energy of the shower enters as a scaling parameter α .

$$\chi^2(x_c, y_c, E, X_{max}) = \sum_{k=1}^4 \left(\frac{V_{\text{exp}}(x_c, y_c, E, X_{max}) - V_{\text{meas}}}{\sigma} \right)^2$$



$$V_{\text{exp}}(x_c, y_c, \alpha \cdot E_0, X_{max}) = \alpha \cdot V_{\text{exp}}(x_c, y_c, E_0, X_{max})$$

Reconstruction of main shower parameters - Method

- RF data + simulations \rightarrow core, energy, X_{max} with 4 antennas.
- Simulation of 60 showers for the virtual array for realistic X_1, X_{max}
 - 40 protons + 20 iron nuclei.
 - known arrival direction from measurement (timing and spectrum).
 - primary energy: 1EeV, fix core (0,0).
- For each core calculate χ^2 .
- Energy of the shower enters as a scaling parameter α .
- Plot $\chi^2 = f(X_{max})$ for all 60 simulations. The minimum of the plot corresponds to reconstructed X_{max} .

$$\chi^2(x_c, y_c, E, X_{max}) = \sum_{k=1}^4 \left(\frac{V_{\text{exp}}(x_c, y_c, E, X_{max}) - V_{\text{meas}}}{\sigma} \right)^2$$

$$V_{\text{exp}}(x_c, y_c, \alpha \cdot E_0, X_{max}) = \alpha \cdot V_{\text{exp}}(x_c, y_c, E_0, X_{max})$$

$$(\chi^2, \alpha, X_{max})_i$$

Test the method with simulated events

- Simulated event true

parameters: $E = 0.8 E_{eV}$,

$\theta = 20^{\circ}$, $\phi = 40^{\circ}$,

primary= p , core

$(x_c = 50m, y_c = -120m)$,

$X_{max} = 720 gr/cm^2$

Test the method with simulated events

Simulated event true

parameters: $E = 0.8 E_{eV}$,

$\theta = 20^\circ$, $\phi = 40^\circ$,

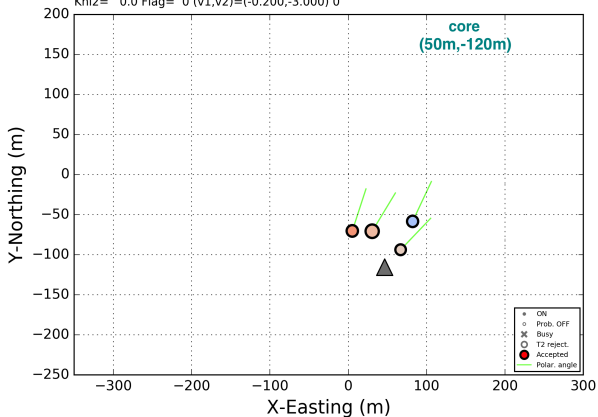
primary=p, core

$(x_c = 50m, y_c = -120m)$,

$X_{max} = 720gr/cm^2$

Coincidences of simulated Event 120617 Multiplicity = No_10_Full

Phi= 40.00 dgr, Theta= 20.00 dgr, T0= 0.0 ns
Khi2= 0.0 Flag= 0 (v1,v2)=(-0.200,-3.000) 0



Test the method with simulated events

Simulated event true

parameters: $E = 0.8 E_{eV}$,

$\theta = 20^\circ$, $\phi = 40^\circ$,

primary= p , core

$(x_c = 50m, y_c = -120m)$,

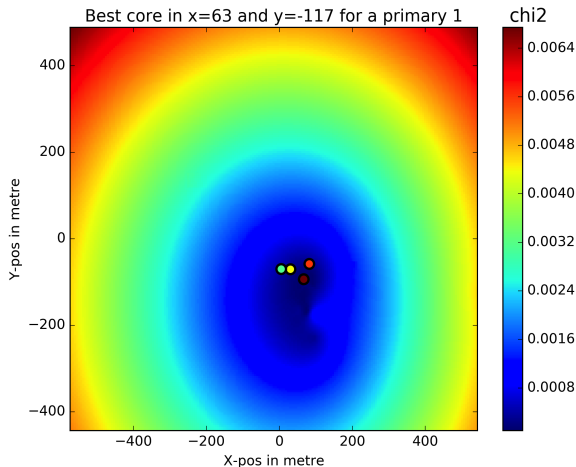
$X_{max} = 720 gr/cm^2$

Reconstructed parameters:

core $(63m, -117m)$,

$E = 0.77 E_{eV}$,

$X_{max} = 713 gr/cm^2$



Test the method with simulated events

- Simulated event true

parameters: $E = 0.8 \text{ EeV}$,

$\theta = 20^\circ$, $\phi = 40^\circ$,

primary= p , core

$(x_c = 50 \text{ m}, y_c = -120 \text{ m})$,

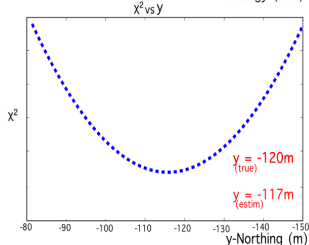
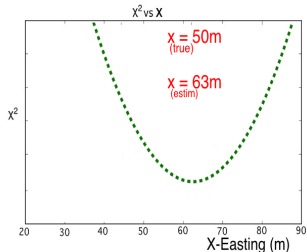
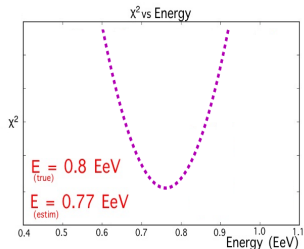
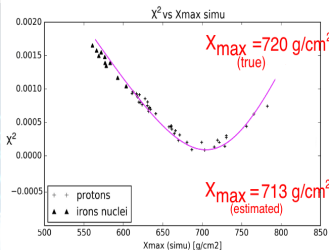
$X_{max} = 720 \text{ gr/cm}^2$

- Reconstructed parameters:

core $(63 \text{ m}, -117 \text{ m})$,

$E = 0.77 \text{ EeV}$,

$X_{max} = 713 \text{ gr/cm}^2$



Test the method with simulated events

- Simulated event true

parameters: $E = 0.8 E_{eV}$,

$\theta = 20^\circ$, $\phi = 40^\circ$,

primary= p , core

($x_c = 50m$, $y_c = -120m$),

$X_{max} = 720 gr/cm^2$

- Reconstructed parameters:

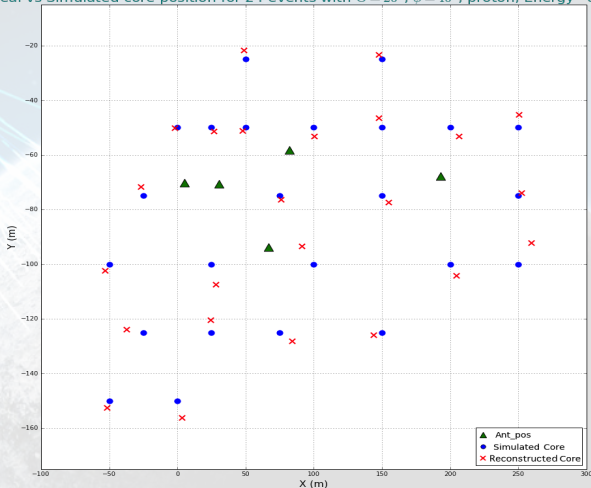
core ($63m$, $-117m$),

$E = 0.77 E_{eV}$,

$X_{max} = 713 gr/cm^2$

- 24 simulated events.

Real vs Simulated core position for 24 events with $\Theta = 20^\circ$, $\phi = 40^\circ$, proton, Energy=0.8EeV



Test the method with simulated events

- Simulated event true

parameters: $E = 0.8 E_{eV}$,

$\theta = 20^\circ$, $\phi = 40^\circ$,

primary= p , core

($x_c = 50m$, $y_c = -120m$),

$X_{max} = 720 gr/cm^2$

- Reconstructed parameters:

core ($63m$, $-117m$),

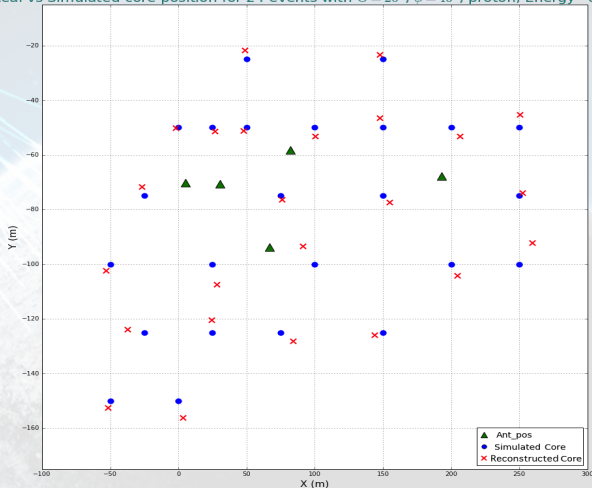
$E = 0.77 E_{eV}$,

$X_{max} = 713 gr/cm^2$

- 24 simulated events.

- The reconstructed core position in good agreement with the simulated.

Real vs Simulated core position for 24 events with $\Theta = 20^\circ$, $\phi = 40^\circ$, proton, Energy=0.8EeV

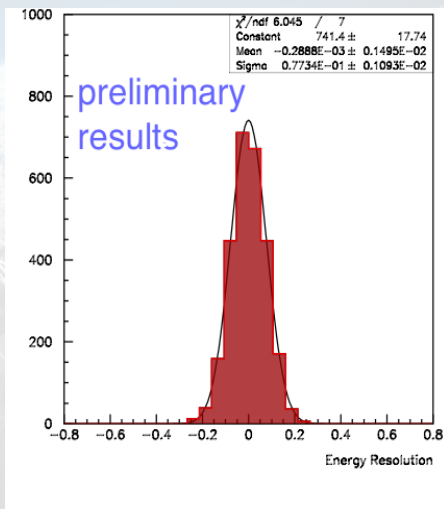


Spatial and energy resolution of the method - work in progress

- Quantify the spatial and energy resolution, estimating the x, y, E for a large number of simulated event (100).

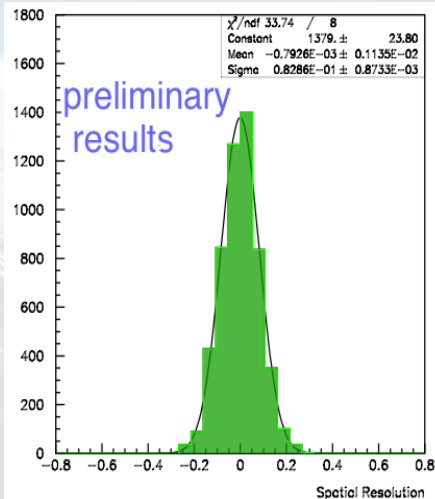
Spatial and energy resolution of the method - work in progress

- Quantify the spatial and energy resolution, estimating the x, y, E for a large number of simulated event (100).
- V_{meas} is obtained again by the simulation but including a smearing of the peak voltage with σ equal to 6% which was estimated by the data (in noise window).
- Preliminary results indicate an energy resolution of 7% and spatial resolution from the station-A center of about 8%.



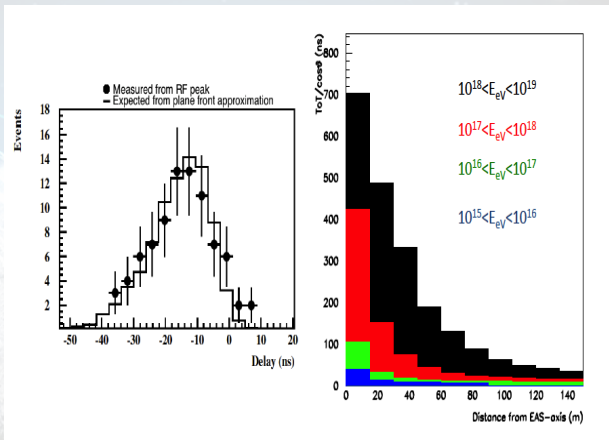
Spatial and energy resolution of the method - work in progress

- Quantify the spatial and energy resolution, estimating the x, y, E for a large number of simulated event (100).
- V_{meas} is obtained again by the simulation but including a smearing of the peak voltage with σ equal to 6% which was estimated by the data (in noise window).
- Preliminary results indicate an energy resolution of 7% and spatial resolution from the station-A center of about 8%.



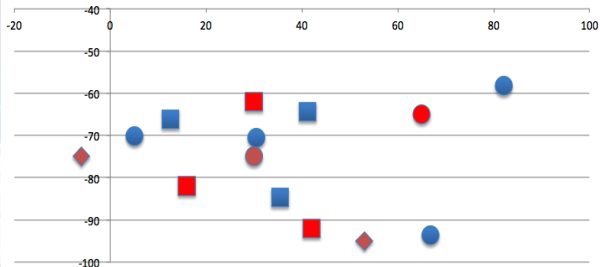
Work in progress

- Efforts is ongoing to include the timing and the charge estimation of the particle detectors to the χ^2 minimization.



Work in progress

- Efforts is ongoing to include the timing and the charge estimation of the particle detectors to the χ^2 minimization.
- The HOU group has designed a low cost station with 3 SDM and 2 RF antennas (3SDM-2RF) station which is under calibration tests. The station is positioned at the same area as station A.



Outline

- 1 Cosmic Rays - Extensive air Showers (EAS)
- 2 Radio Emission
- 3 ASTRONUE Array
- 4 HDM's Performance
- 5 Event Selection-RF Analysis
- 6 Correlation Study and Combined Performance
- 7 Reconstructing EAS direction using RF signal from one antenna
- 8 Core-Energy- X_{max}
- 9 **Conclusions and future work**

Conclusions

- **Confirm that the RF detection in environment with strong electromagnetic noise is possible even with small scale hybrid arrays.**

Conclusions

- **Confirm that the RF detection in environment with strong electromagnetic noise is possible even with small scale hybrid arrays.**
- **RF signal timing at the peak of the EW signal is compatible with the expectation using the HDM pulses timing. This confirm that the RF signal is of cosmic origin.**

Conclusions

- **Confirm that the RF detection in environment with strong electromagnetic noise is possible even with small scale hybrid arrays.**
- **RF signal timing at the peak of the EW signal is compatible with the expectation using the HDM pulses timing. This confirm that the RF signal is of cosmic origin.**
- **The azimuth angle anisotropy agrees with the expectation due to the geomagnetic emission process.**

Conclusions

- **Confirm that the RF detection in environment with strong electromagnetic noise is possible even with small scale hybrid arrays.**
- **RF signal timing at the peak of the EW signal is compatible with the expectation using the HDM pulses timing. This confirm that the RF signal is of cosmic origin.**
- **The azimuth angle anisotropy agrees with the expectation due to the geomagnetic emission process.**
- **The VEL of the antennas which are strongly frequency and angular dependent show that the RF signals spectrum are in agreement with the NEC simulations and MC expectations.**

Conclusions

- **Confirm that the RF detection in environment with strong electromagnetic noise is possible even with small scale hybrid arrays.**
- **RF signal timing at the peak of the EW signal is compatible with the expectation using the HDM pulses timing. This confirm that the RF signal is of cosmic origin.**
- **The azimuth angle anisotropy agrees with the expectation due to the geomagnetic emission process.**
- **The VEL of the antennas which are strongly frequency and angular dependent show that the RF signals spectrum are in agreement with the NEC simulations and MC expectations.**
- **The RF pulse from single antenna combined with MS simulations might give access to the cosmic ray arrival direction.**

Conclusions

- **Confirm that the RF detection in environment with strong electromagnetic noise is possible even with small scale hybrid arrays.**
- **RF signal timing at the peak of the EW signal is compatible with the expectation using the HDM pulses timing. This confirm that the RF signal is of cosmic origin.**
- **The azimuth angle anisotropy agrees with the expectation due to the geomagnetic emission process.**
- **The VEL of the antennas which are strongly frequency and angular dependent show that the RF signals spectrum are in agreement with the NEC simulations and MC expectations.**
- **The RF pulse from single antenna combined with MS simulations might give access to the cosmic ray arrival direction.**
- **Reconstructing core, energy, Xmax and primary mass is feasible with 4 RF antennas and simulations.**

Future Plans

- **Search for low frequency pulses (1-10MHz) from showers.**

Future Plans

- **Search for low frequency pulses (1-10MHz) from showers.**
- **Search for the sudden death pulse.**

Future Plans

- **Search for low frequency pulses (1-10MHz) from showers.**
- **Search for the sudden death pulse.**
- **Efforts from Hellenic Open University group to build a new low cost RF antenna.**

Future Plans

- **Search for low frequency pulses (1-10MHz) from showers.**
- **Search for the sudden death pulse.**
- **Efforts from Hellenic Open University group to build a new low cost RF antenna.**
- **Expand the Astroneu array with more particle detectors and RF antennas. More accurate predictions and extended RF studies.**